**Title**

Laminar Flow on Endothelial Cells Suppresses eNOS O-GlcNAcylation to Promote eNOS Activity

**Permalink**

https://escholarship.org/uc/item/7s98z6d3

**Journal**

Circulation Research, 129(11)

**ISSN**

0009-7330

**Authors**

Basehore, Sarah E
Bohlman, Samantha
Weber, Callie
et al.

**Publication Date**

2021-11-12

**DOI**

10.1161/circresaha.121.318982

Peer reviewed

# Laminar Flow on Endothelial Cells Suppresses eNOS o-GlcNAcylation to Promote eNOS Activity

**Sarah E. Basehore**[1], **Samantha Bohlman**[5], **Callie Weber**[5], **Swathi Swaminathan**[1], **Yuji Zhang**[2], **Cholsoon Jang**[3], **Zoltan Arany**[4], **Alisa Morss Clyne**[5]

[1]School of Biomedical Engineering, Science, and Health Systems, Drexel University, Philadelphia, PA, USA;

[2]Epidemiology and Public Health, University of Maryland School of Medicine, Baltimore, MD, USA;

[3]Biological Chemistry, Chao Family Comprehensive Cancer Center, University of California Irvine, Irvine, CA, USA;

[4]Perelman School of Medicine, University of Pennsylvania, Philadelphia, PA, USA,

[5]Fischell Department of Biomedical Engineering, College of Engineering, University of Maryland, College Park, MD, USA

## Abstract

**Rationale:** In diabetic animals as well as high glucose cell culture conditions, endothelial nitric oxide synthase (eNOS) is heavily O-GlcNAcylated, which inhibits its phosphorylation and nitric oxide (NO) production. It is unknown, however, whether varied blood flow conditions, which affect eNOS phosphorylation, modulate eNOS activity via O-GlcNAcylation-dependent mechanisms.

**Objective:** The goal of this study was to test if steady laminar flow, but not oscillating disturbed flow, decreases eNOS O-GlcNAcylation, thereby elevating eNOS phosphorylation and NO production.

**Methods and Results:** Human umbilical vein endothelial cells (HUVEC) were exposed to either laminar flow (20 dynes/cm$^2$ shear stress) or oscillating disturbed flow (4±6 dynes/cm$^2$ shear stress) for 24 hours in a cone-and-plate device. eNOS O-GlcNAcylation was almost completely abolished in cells exposed to steady laminar but not oscillating disturbed flow. Interestingly, there was no change in protein level or activity of key O-GlcNAcylation enzymes (OGT, OGA, or GFAT). Instead, metabolomics data suggest that steady laminar flow decreases glycolysis and hexosamine biosynthetic pathway (HBP) activity, thereby reducing UDP-GlcNAc pool size and consequent O-GlcNAcylation. Inhibition of glycolysis via 2-deoxy-2-glucose (2-DG) in cells

---

exposed to disturbed flow efficiently decreased eNOS O-GlcNAcylation, thereby increasing eNOS phosphorylation and NO production. Finally, we detected significantly higher O-GlcNAcylated proteins in endothelium of the inner aortic arch in mice, suggesting that disturbed flow increases protein O-GlcNAcylation *in vivo*.

**Conclusions:** Our data demonstrate that steady laminar but not oscillating disturbed flow decreases eNOS O-GlcNAcylation by limiting glycolysis and UDP-GlcNAc substrate availability, thus enhancing eNOS phosphorylation and NO production. This research shows for the first time that O-GlcNAcylation is regulated by mechanical stimuli, relates flow-induced glycolytic reductions to macrovascular disease, and highlights targeting HBP metabolic enzymes in endothelial cells as a novel therapeutic strategy to restore eNOS activity and prevent EC dysfunction in cardiovascular disease.

## Graphical Abstract
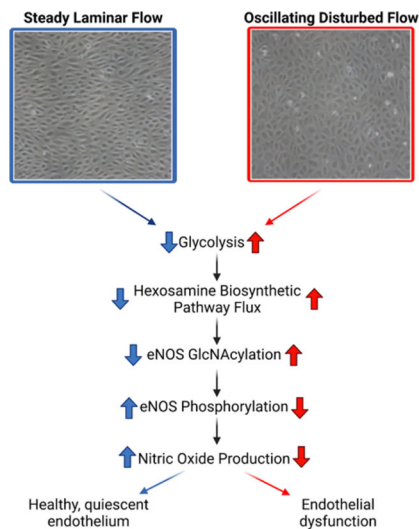


## Abstract

Atherosclerotic plaques are more likely to develop at arterial curvatures and bifurcations where blood flow is disturbed. Endothelial cells in these locations become dysfunctional, characterized by reduced production of nitric oxide. High glucose increases O-GlcNAcylation of endothelial nitric oxide synthase (eNOS) which inhibits its phosphorylation and subsequent generation of nitric oxide. However, eNOS O-GlcNAcylation in endothelial cells exposed to varied flow conditions has not been studied. Our study shows that endothelial cells exposed to laminar flow decrease eNOS O-GlcNAcylation whereas cells exposed to oscillating disturbed flow maintain elevated levels of eNOS O-GlcNAcylation. Decreased eNOS O-GlcNAcylation in laminar flow relates to decreased glycolysis. Indeed, reducing glycolysis in endothelial cells in disturbed flow decreasts eNOS O-GlcNAcylation and increases nitric oxide production. This study shows for the first time that O-GlcNAcylation can be modulated via mechanical stimuli such as shear stress and that glycolytic flux impacts nitric oxide production. Thus, eNOS O-GlcNAcylation could be a potential target for reducing endothelial dysfunction in disturbed flow.

**Subject Terms:**

Atherosclerosis; Endothelium/Vascular Type/Nitric Oxide; Hemodynamics; Metabolism; Vascular Biology

## INTRODUCTION

Cardiovascular disease (CVD) remains the leading cause of death in the United States[1]. CVD is linked to atherosclerotic plaque development in regions of endothelial cell (EC) dysfunction, defined as reduced nitric oxide (NO) bioavailability[2–5]. Metabolic cardiovascular risk factors, including elevated blood glucose, contribute to systemic EC dysfunction[6–11]. Local EC dysfunction occurs at arterial bifurcations and curvatures where the blood flow is disturbed and/or oscillating[12–14].

While EC dysfunction is induced by both metabolic factors and hemodynamic forces, little is known about how hemodynamics regulates EC dysfunction via cell metabolism[12]. *In vitro*, EC glycolytic flux decreased after 72 hours of steady laminar flow through Kruppel-like factor 2 (KLF2)-mediated suppression of 6-phosphofructo-2-kinase/fructose-2,6-biphosphatase 3 (PFKFB3), a rate-limiting glycolytic enzyme[15]. In other studies, mouse and human aortic endothelial cells increased glycolysis in disturbed flow via AMPK and HIF1α[16, 17].

EC metabolism, hemodynamics, and NO bioavailability may be linked via the hexosamine biosynthetic pathway (HBP), a glycolytic side branch responsible for posttranslational glycosylation of around 4,000 proteins[18]. Glucose that enters the cell is converted into fructose-6-phosphate (F6P) during glycolysis. F6P is shunted in the HBP and converted to glucosamine-6-phosphate by the rate limiting enzyme glutamine:fructose-6-phosphate amidotransferase (GFAT). Glucosamine-6-phosphate is then metabolized into UDP-GlcNAc, which acts as the substrate for attachment of *O*-linked N-acetylglucosamine (*O*-GlcNAc) to serine and threonine protein residues. GlcNAc cycles on and off proteins through reactions catalyzed by the O-GlcNAc transferase (OGT) and O-GlcNAcase (OGA), which add and remove GlcNAc, respectively[19].

Torres and Hart first linked O-GlcNAcylation with CVD, showing the small heat shock protein αB-crystallin as a O-GlcNAc target in rat heart[20]. Chronically elevated *O*-GlcNAcylation has since proven important in CVD, particularly in hyperglycemia and diabetes[21–24]. High glucose increased protein GlcNAcylation in human coronary EC, human umbilical vein EC, cardiomyocytes, and homogenized aortic tissue[23, 25–28]. Brownlee *et al.* found that hyperglycemia-associated eNOS inhibition was associated with a twofold increase in eNOS glycosylation through the HBP and a reciprocal decrease in phosphorylation at eNOS serine 1177[29]. Thus eNOS O-GlcNAcylation may be a hallmark of endothelial dysfunction.

While eNOS O-GlcNAcylation and its effect on eNOS phosphorylation has been studied in altered glucose, eNOS O-GlcNAcylation had not yet been studied in flow. We hypothesized that steady laminar but not oscillating disturbed flow decreases eNOS O-GlcNAcylation,

contributing to a quiescent EC phenotype. We now show that eNOS O-GlcNAcylation is decreased in EC adapted to steady laminar flow and decreasing eNOS O-GlcNAcylation in EC exposed to oscillating disturbed flow restores eNOS phosphorylation and NO production. These data suggest that eNOS O-GlcNAcylation may be a target for reducing EC dysfunction in disturbed flow.

## METHODS

### Data Availability.

The data that support the findings of this study are available from the corresponding author upon reasonable request.

### Cell Culture.

HUVEC (passages 5–10, Cell Applications) were cultured in Endothelial Growth Medium-2 (EGM-2; Lonza) supplemented with 10% fetal bovine serum (FBS; HyClone), 1% penicillin-streptomycin, and 1% L-glutamine (Gibco). Human pulmonary artery endothelial cells (hPAEC, passages 6–10) were obtained from the Pulmonary Hypertension Breakthrough Initiative (PHBI) Research Network. hPAEC were cultured in Microvascular Endothelial Growth Medium-2 (EGM-2MV; Lonza) supplemented with 10% FBS, 1% penicillin-streptomycin, and 1% L-glutamine on gelatin-coated (ESGRO 0.1% gelatin, Sigma #SF008) dishes. For flow studies, media was changed to Endothelial Basal Medium-2 (EBM-2; Lonza) supplemented with 10% FBS, 1% penicillin-streptomycin, and 1% L-glutamine 30 minutes prior to shear stress exposure.

### Reagents.

A small molecule OGA inhibitor, NButGT, was a generous gift from Dr. Mauricio Reginato (Drexel University, College of Medicine). A small molecule OGT inhibitor, $(OAc)_4$5S-GlcNAc, was a generous gift from Dr. David Vocadlo (Simon Fraser University, Chemical Biology). Azaserine (GFAT inhibitor) was obtained from Cayman chemical (115-02-6)[30]. 2-deoxy-D-glucose (2-DG) was obtained from Sigma (D8375)[31].

### Shear Stress Exposure.

For flow studies, a custom-built cone-and-plate device was used to apply shear stress to HUVEC (Figure 1)[32]. If the modified Reynolds number and cone angle are small, the shear stress is determined from the equation

$$\tau_w = \frac{\mu\omega}{\alpha} \qquad (1)$$

where μ is fluid dynamic viscosity, ω is cone angular velocity, and α is cone angle[33, 34]. For steady laminar flow, the cone rotated at 420 RPM, producing 20 dynes/cm$^2$ shear stress[33]. For oscillating disturbed flow, the cone rotated in an oscillatory manner to produce 4±6 dynes/cm$^2$ shear stress as:

$$\omega(t) = 7\frac{rad}{s} + \left(10.5 \quad \frac{rad}{s}\right)\sin(2\pi ft) \tag{2}$$

where the amplitude shift 7 rad/s (85 RPM) equates to 4 dynes/cm$^2$ and the sine wave amplitude 10.5 rad/s (126 RPM) equates to 6 dynes/cm$^2$. Frequency was set at 1 Hz.

For each experiment, 17,000 cells/cm$^2$ were seeded on a collagen Type 1 coated dish. Cells were cultured for 48 hours and then assembled into the cone and plate device in a 37°C, 5% $CO_2$ incubator. Samples cultured in static conditions in the same incubator or samples exposed to the same flow conditions without the applied inhibitor were used as controls.

### Western Blot and Immunoprecipitation.

Protein levels were determined by Western blot as described[35]. For immunoprecipitation, eNOS primary antibody (1:100, 9586 Cell Signaling) was added to cell lysates overnight at 4°C. Protein A agarose beads (1:10, Cell Signaling) were then added to the solution for 3 hours at 4°C. Samples were then centrifuged for 30 seconds at 2,000g, after which the pelleted bead-antibody-protein complexes were thoroughly washed. Finally, SDS sample buffer was added, samples were centrifuged for 30 seconds at 2,000g, and the supernatant was then analyzed by Western blot[36]. Antibody specificity was checked with positive controls, and O-GlcNAc antibody specificity was further confirmed by demonstrating reduced protein O-GlcNAcylation in Western blots of cells incubated with O-GlcNAcase. Membranes were incubated with primary antibodies for GlcNAc CDT110.6 (9875S), OGT (24083), p-eNOS (9570S), eNOS (9572S), PFKFB3 (13123S), GFAT1 (5322, all from Cell Signaling) as well as OGA (SAB4200267 Sigma), p-GFAT (28123, Takara), Na$^+$/K$^+$/ATPase (sc-28800, Santa Cruz), and caveolin-1 (sc-70516, Santa Cruz) at 1:1000 dilution overnight at 4°C followed by the appropriate secondary horseradish peroxidase-conjugated antibody (1:2000, Promega) for 1 hour at room temperature. GAPDH (437000, ThermoFisher) or β-actin (SC47778-C4, Santa Cruz) were used as the loading control. Protein bands were detected using an enhanced chemiluminescence kit (Western Lightning, PerkinElmer) and visualized with a Fluorchem digital imager (Alpha Innotech). Band intensity was quantified using AlphaEase FC software and normalized to both the control protein and a specific condition on each blot to combine samples across Western blots.

### siRNA Transfection.

HUVEC were transfected with siRNA as per the Ambion siRNA silencer select transfection protocol (ThermoFisher) using human eNOS silencer select siRNA (ThermoFisher, #4392420), negative control #1 (Thermofisher, #4390843) and GAPDH (ThermoFisher, #4390849).

### OGT and OGA Activity.

HUVEC OGA activity was analyzed via an OGA activity kit (BMR) as per manufacturer instructions. HUVEC OGT activity was analyzed via the UDP-Glo Glycosyltransferase Assay (Promega) as per manufacturer instructions.

### Mass Spectrometry.

Endothelial metabolites were measured via liquid chromatography mass spectrometry (LC-MS). HUVEC were exposed to different flow conditions for 24 hours as described. After flow, 5 mM U-$^{13}C_6$-glucose (Cambridge Isotope Laboratories, CLM-1396) in glucose, glutamine, and pyruvate free DMEM (ThermoFisher, A14430–01) supplemented with 10% FBS, 1% penicillin-streptomycin, and 1% L-glutamine was added for two minutes. Media was then removed from cells and 80:20 methanol:water (−80°C, extraction solvent) was added to cells for 15 minutes at −80°C. Cells were scraped in the extraction solvent and cell lysates pipetted into Eppendorf tubes. Samples were centrifuged at 16,000g for 10 minutes at 4°C to pellet debris. The supernatant was transferred to a new tube, desiccated under nitrogen gas flow, and re-dissolved in LC-MS grade water. Metabolites were analyzed via reverse-phase ion-pairing chromatography coupled to an Exactive Orbitrap mass spectrometer (ThermoFisher, San Jose, CA) following an established protocol[37].

### Nitric Oxide (NO) Production.

NO production in HUVEC was measured via Griess Assay (Thermofisher Scientific, G7921), DAF-FM Diacetate (Thermofisher Scientific, D23844), and a Zysense 280 NO analyzer. For DAF-FM, HUVEC were incubated with 1:1000 DAF-FM in EBM-2 medium for 30 minutes at 37°C. Cells were then fixed with 4% paraformaldehyde, mounted using Prolong Gold Antifade (Thermofisher Scientific, P36930), and imaged with a Zeiss LSM700 confocal microscope. For the NO analyzer, sample media was collected after flow exposure and centrifuged at 13,000 g for 5 minutes. 200 μL of supernatant was then added to the NO analyzer. Voltage readings were normalized to baseline, and the area under the peak was used to determine nitrite levels using a standard curve. Each sample was measured at least three times.

### Ex vivo vessel analysis.

C57BL/6 mice (Jackson Laboratories, Bar Harbor, ME) were allowed free access to standard food and water. All animal experiments were conducted in accordance with NIH policies and were approved by the Drexel University Institutional Animal Care and Use Committee (IACUC). No animals were excluded from the analyses. 10-week old male mice were euthanized using ketamine/xylazine cocktail followed by a secondary thoracotomy. The descending aorta and aortic arch were removed, fixed overnight in 4% paraformaldehyde, and embedded in 50:50 OCT-Sucrose. 5 μm aortic cross-sections were blocked and then incubated with an O-GlcNac (Biolegend, 838004, 1:100) or ICAM-1 (ThermoFisher, MA119123, 1:100) antibody overnight at 4°C. Samples were incubated with an AlexaFluor 488 (ThermoFisher, A-21121, 1:100) or AlexaFluor 594 (ThermoFisher, A-11001 1:100) goat anti-mouse secondary antibody. Finally, samples were mounted in Permount and imaged using a Zeiss LSM 700 microscope (63X, maximum intensity projection). While data from male mice are presented, we observed similar results in 5-month-old female C57BL/6J mice.

### Statistical Analysis.

Statistical analysis was performed with GraphPad Prism. Non-parametric statistical tests were used in all cases in which the sample number was too low to demonstrate normality. All analyses were corrected for multiple comparisons. The statistical tests used to analyze each data set are provided in the figure captions. Where possible (activity assays, mass spectrometry, NO quantification, confocal microscopy), the researcher was blinded during analysis through the use of random sample numbers. Representative images were selected as those that best represented the mean of the quantified data.

## RESULTS

### Steady laminar flow, but not oscillating disturbed flow reduced eNOS O-GlcNAcylation.

We first sought to determine the fidelity of our cone and plate flow device to mimic laminar and disturbed flow regimes (Figure 1A,B). ECs exposed to 24 hours of steady laminar flow aligned and elongated with the flow direction whereas cells exposed to 24 hours of oscillating disturbed flow remained in a cobblestone architecture (Figure 1C). Furthermore, ECs exposed to 24 hours of steady laminar flow increased phosphorylated eNOS as compared to cells in static culture ($p = 1.00 \times 10^{-2}$ by Kruskal-Wallis test; Figure 1D), leading to nearly twice as much NO as compared to cells in static culture or oscillating disturbed flow ($p = 2.10 \times 10^{-4}$ by Kruskal-Wallis test; Figure 1E). These results are consistent with previously reported EC phenotypes under different blood flow conditions and thus indicate effective modeling of flow exposure with our device.

We then measured protein O-GlcNAcylation in ECs exposed to flow. Total protein O-GlcNAcylation was unchanged among ECs exposed to 24 hours of static culture, steady laminar, or oscillating disturbed flow ($p = 8.78 \times 10^{-1}$ by one-way ANOVA; Figure 2A); however, O-GlcNAcylation of a single protein band ~140 kDa (black arrow) nearly disappeared in HUVEC exposed to steady laminar flow as compared to static culture and oscillating disturbed flow ($p = 1.84 \times 10^{-11}$ by one-way ANOVA; Figure 2A). This change was observed as early as 3 hours after flow initiation (Online Figure III). O-GlcNAcylation of the 140 kDa protein was not reduced in EC exposed to oscillating disturbed flow when compared to cells in static culture (Figure 2A). We similarly observed decreased O-GlcNAcylation of the 140 kDa protein in human pulmonary artery endothelial cells exposed to 24 hours of steady laminar flow (Online Figure II).

Since eNOS molecular weight is ~140 kDa, and the single demonstrated eNOS O-GlcNAcylation site (~200 Da) does not significantly change protein molecular weight, we hypothesized that the protein with reduced O-GlcNAcylation was eNOS[18]. We therefore knocked down eNOS using siRNA in cells in static culture (Figure 2B). When these cells were analyzed by Western blot, both the eNOS band and the O-GlcNAc band at ~140 kDa were drastically reduced. To further verify that the ~140 kDa protein was eNOS, eNOS was immunoprecipitated from the lysates of HUVEC exposed to static culture or steady laminar flow for 24 hours (Figure 2C). EC exposed to oscillating disturbed flow were not included in this experiment so samples could be analyzed as quickly as possible. Both the total protein and immunoprecipitated eNOS samples showed decreased protein O-GlcNAcylation at ~140

kDa in cells exposed to laminar flow compared to cells in static culture. These data suggest that the ~140 kDa protein that was not O-GlcNAcylated in steady laminar flow was eNOS.

### OGT and OGA did not change in steady laminar flow, but modulating OGT and OGA affected eNOS phosphorylation.

We then investigated the mechanism by which eNOS O-GlcNAcylation decreased in steady laminar but not oscillating disturbed flow. We measured flow-induced changes in the enzymes OGT and OGA, including protein quantity and activity. OGT and OGA protein quantity were unchanged in HUVEC exposed to static culture, steady laminar flow, and oscillating disturbed flow (Figure 3A).

Finally, we quantified OGT and OGA activity. Since we observed a decrease in O-GlcNAcylated eNOS after 3 hours of steady laminar flow, we measured OGT and OGA activity up to two hours after flow initiation, assuming an enzymatic change would occur prior to a change in O-GlcNAcylated eNOS. OGT activity remained unchanged in HUVEC exposed to up to 2 hours of laminar flow whereas OGA activity decreased after 2 hours (Figure 3B). These data suggest that OGA activity may be decreased by steady laminar flow; however, protein O-GlcNAcylation would be expected to increase with decreased OGA activity. Therefore, neither OGT nor OGA were likely mechanisms for decreased eNOS O-GlcNAcylation in EC exposed to steady laminar flow.

We then determined whether we could alter eNOS phosphorylation in HUVEC adapted to steady laminar or oscillating disturbed flow by modulating eNOS O-GlcNAcylation via OGT and OGA. We exposed HUVEC to steady laminar flow with an OGA inhibitor (Figure 3C). The OGA inhibitor doubled eNOS O-GlcNAcylation in laminar flow (p = $2.99\times10^{-3}$ by Mann-Whitney test); eNOS phosphorylation also decreased, but the effect was not statistically significant. We also exposed HUVEC to oscillating disturbed flow with an OGT inhibitor. The OGT inhibitor decreased eNOS O-GlcNAcylation in disturbed flow (p = $3.79\times10^{-2}$ by Mann-Whitney test) as well as increased eNOS phosphorylation (p = $8.30\times10^{-2}$ by Mann-Whitney test). Neither OGA nor OGT inhibition changed eNOS protein levels.

### Decreased HBP flux and UDP-GlcNAc may contribute to decreased eNOS O-GlcNAcylation in steady laminar flow.

Since protein O-GlcNAcylation depends on UDP-GlcNAc substrate availability, we next measured HBP flux by U-$^{13}C_6$-glucose mass spectrometry. UDP-GlcNAc decreased ~60% in EC exposed to steady laminar flow as compared to static culture and oscillating disturbed flow (p = $9.79\times10^{-6}$ by Kruskal-Wallis with Dunn's multiple comparisons test; Figure 4A). However, GFAT protein and phosphorylation did not change in EC exposed to steady laminar flow as compared to static culture, while GFAT phosphorylation did increase slightly in endothelial cells exposed to oscillating disturbed flow (Figure 4B). These results suggest that decreased HBP flux in EC exposed to steady laminar flow contributed to decreased UDP-GlcNAc substrate availability, causing decreased eNOS O-GlcNAcylation. We then examined whether inhibiting HBP flux could decrease eNOS O-GlcNAcylation in oscillating disturbed flow. When GFAT was inhibited in HUVEC using azaserine,

UDP-GlcNAc also decreased 50% (p = $2.16 \times 10^{-3}$ by Mann-Whitney test; Figure 4A), eNOS O-GlcNAcylation decreased 80% (p = $2.34 \times 10^{-2}$ by Kruskal-Wallis test; Figure 4C,), and eNOS phosphorylation increased 50% (p = $3.39 \times 10^{-2}$ by Kruskal-Wallis test). Thus decreasing HBP activity via GFAT inhibition decreased eNOS O-GlcNAcylation and subsequently increased eNOS phosphorylation.

HBP is a key glycolytic branch pathway[38]. We therefore investigated whether reduced glycolytic flux in HUVEC exposed to steady laminar flow could contribute to decreased eNOS O-GlcNAcylation. When HUVEC exposed to static culture, steady laminar flow, or oscillating disturbed flow were analyzed by metabolic mass spectrometry after 2 minutes of U-$^{13}$C$_6$-glucose labeling (Figure 5A), the labeled percentage of intracellular glucose and glycolytic intermediates such as fructose-6-phosphate and glyceraldehyde-3-phosphate was significantly lower in HUVEC exposed to steady laminar flow as compared to static culture or oscillating disturbed flow. Lactate remained almost entirely unlabeled at 2 minutes, indicating that the labeled glucose was still progressing through glycolysis at that time point.

We then investigated whether decreasing glycolysis via 2-DG could inhibit eNOS O-GlcNAcylation. When HUVEC were exposed to 24 hours of oscillating disturbed flow with 2-DG, O-GlcNAcylated eNOS decreased by 60% (p = $2.44 \times 10^{-2}$ by Mann-Whitney test; Figure 5B), eNOS phosphorylation increased by 50% (p = $4.22 \times 10^{-2}$ by Mann-Whitney test Figure 5B). Nitrite also increased, although the change was not statistically significant (Figure 5C). DAF-FM confocal microscopy (p = $2.89 \times 10^{-2}$ by Mann-Whitney test; Figure 5D) and Zysense NO analyzer (p = $2.80 \times 10^{-3}$ by Mann-Whitney test; Figure 5E) confirmed increased NO in HUVEC exposed to disturbed flow with 2-DG. These data suggest that decreasing glycolysis in EC exposed to oscillating disturbed flow can decrease eNOS O-GlcNAcylation, increase eNOS phosphorylation, and increase NO.

### Protein O-GlcNAcylation was lower in atheroprotected aortic regions.

To investigate whether protein O-GlcNAcylation decreased in laminar vs. disturbed flow vascular regions *in vivo*, we compared aortic regions in C57BL/6J mice (Figure 6C). Healthy mice on a standard diet were used since eNOS O-GlcNAcylation was previously shown to increase in diabetic animals[29], and our prior studies suggest that hyperglycemia inhibits endothelial shear stress response and thereby might abrogate O-GlcNAcylation differences with steady laminar vs. oscillating disturbed flow[39–41]. The endothelium in the inner aortic arch of 10 week old male C57BL/6J mice, which are atheroprone due to lower wall shear stress and higher oscillatory index (disturbed flow), showed higher protein O-GlcNAcylation (green) compared to the outer aortic arch and the descending aorta (p = $1.60 \times 10^{-3}$ by Kruskal-Wallis with Dunn's multiple comparisons test; Figure 6A), which are atheroprotected due to higher wall shear stress and lower oscillatory index[42–44]. We similarly observed increased EC ICAM-1 in the inner aortic arch as compared to the outer aortic arch and descending aorta, confirming our EC labeling and matching with reports of increased inflammation in disturbed flow aortic regions (Figure 6B). These data suggest that protein O-GlcNAcylation increases in endothelium in atheroprone areas of disturbed flow *in vivo*.

## DISCUSSION

eNOS O-GlcNAcylation increases in high glucose, which decreases eNOS phosphorylation and subsequent NO production[23, 24, 26, 27, 29, 45–48]. We now show that eNOS O-GlcNAcylation decreases in steady laminar flow but not in oscillating disturbed flow, which may contribute to altered eNOS phosphorylation and NO production in these flow regimes. These changes did not relate to altered OGT, OGA, or GFAT but instead appear to relate to decreased glycolytic and HBP flux. Our data further suggest that eNOS O-GlcNAcylation and phosphorylation can be modulated in EC exposed to oscillating disturbed flow through glycolysis inhibitors. Thus eNOS O-GlcNAcylation is a potential target for reducing endothelial dysfunction and subsequent atherosclerosis in disturbed flow areas[14].

Our research shows both *in vitro* and *in vivo* that hemodynamic shear stress modulates protein O-GlcNAcylation. Prior to our study, only biochemical stimuli such as high glucose were shown to increase HBP activity and protein O-GlcNAcylation. Since protein O-GlcNAcylation is a sensor of biochemical metabolic and stress stimuli[49], our data suggest a link connecting hemodynamics, metabolic stress, and macrovascular EC dysfunction. Thus our work expands the impact of prior studies linking biomechanical stimuli such as shear stress and substrate stiffness to metabolic changes[15–17, 50–52] by relating metabolic changes to EC NO bioavailability.

eNOS O-GlcNAcylation in disturbed flow could be a therapeutic target. While OGT inhibition decreased eNOS O-GlcNAcylation, not all OGT inhibitors are suitable for use *in vivo*, mostly due to poor solubility in aqueous solutions[53]. 2-DG has been used to suppress cancer tumors *in vivo*[54–57]. In addition to inhibiting glycolysis, 2-DG phosphorylated GFAT1 at Ser243 via ATP associated-AMPK activation, effectively decreasing GFAT activity in CHO-IR and HEK293 cells[58]. Thus 2-DG could decrease eNOS O-GlcNAcylation by reducing glycolysis and GFAT activity. Since EC protein O-GlcNAcylation is essential for cell function and could not be systemically inhibited, an O-GlcNAc therapy could be targeted to ICAM-1 for example, which is elevated in endothelium exposed to oscillating disturbed flow[59–61].

The specific site at which eNOS is O-GlcNAcylated remains uncertain. Prior studies suggested but did not show that eNOS O-GlcNAcylation occurred at the Ser1177 phosphorylation site[24, 62, 63]. When we analyzed eNOS by mass spectrometry, we could not detect high confidence O-GlcNAc sites. Recently, Aulak *et al* observed increased eNOS O-GlcNAcylation and decreased eNOS Ser1177 phosphorylation in endothelial cells from patients with pulmonary artery hypertension[64]. Since they were similarly unable to purify enough endothelial eNOS to determine the O-GlcNAc modification site by mass spectrometry, they overexpressed eNOS and OGT in bacteria. Their mass spectrometry revealed that eNOS was O-GlcNAcylated at Ser615, and mutating eNOS at this site reduced its O-GlcNAcylation. They hypothesize that changes in eNOS Ser615, which is in the eNOS auto-inhibitory loop, may alter the position or accessibility of Ser1177 for phosphorylation and activation.

Author Manuscript

Author Manuscript

Author Manuscript

Author Manuscript

While our study shows that O-GlcNAcylation decreases in areas of laminar flow both *in vitro* and *in vivo*, it is not without limitations. We showed protein but not eNOS O-GlcNAcylation in mouse aortae due to antibody limitations. Since the O-GlcNAc antibody also binds to *O*-GlcNAcylated cell surface proteins, some observed *in vivo* changes could relate to the endothelial glycocalyx[65]. However, the glycocalyx should be thinner at the inner aortic arch and thicker at the outer aortic arch[66, 67]. We used chemical OGA and OGT inhibitors since HUVEC did not survive in flow following OGA or OGT siRNA knockdown. Chemical inhibitors allowed us to titrate inhibition and investigate possible therapies. However, chemical inhibitors may have short half-lives, partial inhibition, and off target effects. OGA and OGT also control *O*-GlcNAcylation of many cell proteins, including those that affect caveolae[68]. We found that modulating caveolae either through methyl-β-cyclodextran or siRNA caveolin-1 knockdown could change eNOS O-GlcNAcylation, although not the laminar-flow induced decrease in eNOS O-GlcNAcylation (Online Figure I).

In conclusion, our study shows that shear stress regulates eNOS O-GlcNAcylation, affecting eNOS phosphorylation and subsequent NO production. Our data suggest eNOS O-GlcNAcylation is inhibited by decreased glycolytic activity, which reduces UDP-GlcNAc availability. Reducing eNOS O-GlcNAcylation via OGT, GFAT, and glycolysis inhibitors increase eNOS phosphorylation and subsequent NO production. Overall, our data demonstrate that eNOS O-GlcNAcylation is a potential target for endothelial dysfunction in CVD.

## Supplementary Material

Refer to Web version on PubMed Central for supplementary material.

## ACKNOWLEDGEMENTS

### SOURCES OF FUNDING

## Nonstandard Abbreviations and Acronyms:

| | |
|---|---|
| **CVD** | cardiovascular disease |
| **EC** | endothelial cells |
| **NO** | nitric oxide |
| **eNOS** | endothelial nitric oxide synthase |
| **HUVEC** | human umbilical vein endothelial cells |
| **HBP** | hexosamine biosynthetic pathway |

| **O-GlcNAc** | *O*-linked N-acetylglucosamine |
|---|---|
| **OGT** | protein O-GlcNAc transferase |
| **OGA** | protein O-GlcNAcase |
| **GFAT** | glucosamine-fructose-6-phosphate aminotransferase |

## REFERENCES

1. Zibrova D, Vandermoere F, Goransson O, Peggie M, Marino KV, Knierim A, Spengler K, Weigert C, Viollet B, Morrice NA, Sakamoto K, Heller R. Gfat1 phosphorylation by ampk promotes vegf-induced angiogenesis. Biochem. J 2017;474:983–1001 [PubMed: 28008135]

2. Michiels C Endothelial cell functions. J. Cell. Physiol 2003;196:430–443 [PubMed: 12891700]

3. Harrison DG. Cellular and molecular mechanisms of endothelial cell dysfunction. The Journal of clinical investigation. 1997;100:2153–2157 [PubMed: 9410891]

4. Shimokawa H Primary endothelial dysfunction: Atherosclerosis. J. Mol. Cell. Cardiol 1999;31:23–37 [PubMed: 10072713]

5. Kawashima S, Yokoyama M. Dysfunction of endothelial nitric oxide synthase and atherosclerosis. Atertio. Thromb. Vasc. Biol 2004;24:998–1005

6. Cybulsky MI, Gimbrone MA, Jr. Endothelial expression of a mononuclear leukocyte adhesion molecule during atherogenesis. Science. 1991;251:788–791 [PubMed: 1990440]

7. Osborn L, Hession C, Tizard R, Vassallo C, Luhowskyj S, Chi-Rosso G, Lobb R. Direct expression cloning of vascular cell adhesion molecule 1, a cytokine-induced endothelial protein that binds to lymphocytes. Cell. 1989;59:1203–1211 [PubMed: 2688898]

8. van den Born B-JH, Löwenberg EC, van der Hoeven NV, de Laat B, Meijers JC, Levi M, van Montfrans GA. Endothelial dysfunction, platelet activation, thrombogenesis and fibrinolysis in patients with hypertensive crisis. J. Hypertens 2011;29:922–927 [PubMed: 21372741]

9. Hennig B, Chow CK. Lipid peroxidation and endothelial cell injury: Implications in atherosclerosis. Free Radical Biol. Med 1988;4:99–106 [PubMed: 3278952]

10. Tsai J-C, Perrella MA, Yoshizumi M, Hsieh C-M, Haber E, Schlegel R, Lee M-E. Promotion of vascular smooth muscle cell growth by homocysteine: A link to atherosclerosis. Proceedings of the National Academy of Sciences. 1994;91:6369–6373

11. Mestas J, Ley K. Monocyte-endothelial cell interactions in the development of atherosclerosis. Trends Cardiovasc. Med 2008;18:228–232 [PubMed: 19185814]

12. Chiu JJ, Chien S. Effects of disturbed flow on vascular endothelium: Pathophysiological basis and clinical perspectives. Physiol. Rev 2011;91:327–387 [PubMed: 21248169]

13. Adel M Malek M, Seth L. Alper, Seigo Izumo. Hemodynamic shear stress and its role in atherosclerosis. JAMA. 1999;282:2035–2042 [PubMed: 10591386]

14. Yetik-Anacak G, Catravas JD. Nitric oxide and the endothelium: History and impact on cardiovascular disease. Vascul. Pharmacol 2006;45:268–276 [PubMed: 17052961]

15. Doddaballapur A, Michalik KM, Manavski Y, Lucas T, Houtkooper RH, You X, Chen W, Zeiher AM, Potente M, Dimmeler S, Boon RA. Laminar shear stress inhibits endothelial cell metabolism via klf2-mediated repression of pfkfb3. Arterioscler. Thromb. Vasc. Biol 2015;35:137–145 [PubMed: 25359860]

16. Wu D, Huang RT, Hamanaka RB, Krause M, Oh MJ, Kuo CH, Nigdelioglu R, Meliton AY, Witt L, Dai G, Civelek M, Prabhakar NR, Fang Y, Mutlu GM. Hif-1alpha is required for disturbed flow-induced metabolic reprogramming in human and porcine vascular endothelium. Elife 2017;6

17. Yang Q, Xu J, Ma Q, Liu Z, Sudhahar V, Cao Y, Wang L, Zeng X, Zhou Y, Zhang M, Xu Y, Wang Y, Weintraub NL, Zhang C, Fukai T, Wu C, Huang L, Han Z, Wang T, Fulton DJ, Hong M, Huo Y. Prkaa1/ampkalpha1-driven glycolysis in endothelial cells exposed to disturbed flow protects against atherosclerosis. Nat Commun. 2018;9:4667 [PubMed: 30405100]

18. Ma J, Hart GW. O-glcnac profiling: From proteins to proteomes. Clin. Proteomics 2014;11:8–8 [PubMed: 24593906]

19. Bond MR, Hanover JA. A little sugar goes a long way: The cell biology of o-glcnac. J. Cell Biol 2015;208:869–880 [PubMed: 25825515]

20. Torres C-R, Hart, Gerald W. Topography and polypeptide distribution of terminal n-acetylglucosamine residues on the surfaces of intact lymphocytes. Evidence for o-linked glcnac. The Journal of biological chemistry. 1984;259:3308–3317 [PubMed: 6421821]

21. Karunakaran U, Jeoung NH. O-glcnac modification: Friend or foe in diabetic cardiovascular disease. Korean Diabetes J. 2010;34:211–219 [PubMed: 20835337]

22. Mäkimattila S, Virkamäki A, Groop PH, Cockcroft J, Utriainen T, Fagerudd J, Yki-Järvinen H. Chronic hyperglycemia impairs endothelial function and insulin sensitivity via different mechanisms in insulin-dependent diabetes mellitus. Circulation. 1996;94:1276–1282 [PubMed: 8822980]

23. Medford HM, Chatham JC, Marsh SA. Chronic ingestion of a western diet increases o-linked-beta-n-acetylglucosamine (o-glcnac) protein modification in the rat heart. Life Sci. 2012;90:883–888 [PubMed: 22575823]

24. Musicki B, Kramer MF, Becker RE, Burnett AL. Inactivation of phosphorylated endothelial nitric oxide synthase (ser-1177) by o-gicnac in diabetes-associated erectile dysfunction. Proc. Natl. Acad. Sci. U. S. A 2005;102:11870–11875 [PubMed: 16085713]

25. Marsh SA, Dell'Italia LJ, Chatham JC. Activation of the hexosamine biosynthesis pathway and protein o-glcnacylation modulate hypertrophic and cell signaling pathways in cardiomyocytes from diabetic mice. Amino Acids. 2011;40:819–828 [PubMed: 20676904]

26. Federici M, Menghini R, Mauriello A, Hribal ML, Ferrelli F, Lauro D, Sbraccia P, Spagnoli LG, Sesti G, Lauro R. Insulin-dependent activation of endothelial nitric oxide synthase is impaired by o-linked glycosylation modification of signaling proteins in human coronary endothelial cells. Circulation. 2002;106:466–472 [PubMed: 12135947]

27. Clark RJ, McDonough PM, Swanson E, Trost SU, Suzuki M, Fukuda M, Dillmann WH. Diabetes and the accompanying hyperglycemia impairs cardiomyocyte calcium cycling through increased nuclear o-glcnacylation. J. Biol. Chem 2003;278:44230–44237 [PubMed: 12941958]

28. Hu Y, Belke D, Suarez J, Swanson E, Clark R, Hoshijima M, Dillmann Wolfgang H. Adenovirus-mediated overexpression of o-glcnacase improves contractile function in the diabetic heart. Circul. Res 2005;96:1006–1013

29. Du XL, Edelstein D, Dimmeler S, Ju QD, Sui C, Brownlee M. Hyperglycemia inhibits endothelial nitric oxide synthase activity by posttranslational modification at the akt site. J. Clin. Invest 2001;108:1341–1348 [PubMed: 11696579]

30. Wu GE Haynes T, Li H, Yan W, Meininger C. Glutamine metabolism to glucosamine is necessary for glutamine inhibition of endothelial nitric oxide synthesis. 2001.

31. Wang Q, Liang B, Shirwany NA, Zou M-H. 2-deoxy-d-glucose treatment of endothelial cells induces autophagy by reactive oxygen species-mediated activation of the amp-activated protein kinase. PLoS One. 2011;6:e17234 [PubMed: 21386904]

32. Brown TD. Techniques for mechanical stimulation of cells in vitro. J. Biomech 2000;33:3–14 [PubMed: 10609513]

33. Buschmann MH, Dieterich P, Adams NA, Schnittler HJ. Analysis of flow in a cone-and-plate apparatus with respect to spatial and temporal effects on endothelial cells. Biotechnol. Bioeng 2005;89:493–502 [PubMed: 15648084]

34. Bussolari SR. Apparatus for subjecting living cells to fluid shear stress. Rev. Sci. Instrum 1982;53:1851 [PubMed: 7156852]

35. Mathew JG, Basehore S, Clyne AM. Fluid shear stress and fibroblast growth factor-2 increase endothelial cell-associated vitronectin. Appl. Bionics Biomech 2017;2017:9040161 [PubMed: 28659710]

36. Fulton D, Church JE, Ruan L, Li C, Sood SG, Kemp BE, Jennings IG, Venema RC. Src kinase activates endothelial nitric-oxide synthase by phosphorylating tyr-83. J. Biol. Chem 2005;280:35943–35952 [PubMed: 16123043]

37. Jang C, Hui S, Lu W, Cowan AJ, Morscher RJ, Lee G, Liu W, Tesz GJ, Birnbaum MJ, Rabinowitz JD. The small intestine converts dietary fructose into glucose and organic acids. Cell Metab. 2018;27:351–361.e353 [PubMed: 29414685]

38. Chaveroux C, Sarcinelli C, Barbet V, Belfeki S, Barthelaix A, Ferraro-Peyret C, Lebecque S, Renno T, Bruhat A, Fafournoux P. Nutrient shortage triggers the hexosamine biosynthetic pathway via the gcn2-atf4 signalling pathway. Sci. Rep 2016;6:27278 [PubMed: 27255611]

39. Kemeny SF, Cicalese S, Figueroa DS, Clyne AM. Glycated collagen and altered glucose increase endothelial cell adhesion strength. J. Cell. Physiol 2013;228:1727–1736 [PubMed: 23280505]

40. Kemeny SF, Figueroa DS, Andrews AM, Barbee KA, Clyne AM. Glycated collagen alters endothelial cell actin alignment and nitric oxide release in response to fluid shear stress. J. Biomech 2011;44:1927–1935 [PubMed: 21555127]

41. Kemeny SF, Figueroa DS, Clyne AM. Hypo- and hyperglycemia impair endothelial cell actin alignment and nitric oxide synthase activation in response to shear stress. PLoS One. 2013;8:e66176 [PubMed: 23776627]

42. VanderLaan PA, Reardon CA, Getz GS. Site specificity of atherosclerosis: Site-selective responses to atherosclerotic modulators. Arterioscler. Thromb. Vasc. Biol 2004;24:12–22 [PubMed: 14604830]

43. Feintuch A, Ruengsakulrach P, Lin A, Zhang J, Zhou YQ, Bishop J, Davidson L, Courtman D, Foster FS, Steinman DA, Henkelman RM, Ethier CR. Hemodynamics in the mouse aortic arch as assessed by mri, ultrasound, and numerical modeling. Am. J. Physiol. Heart Circ. Physiol 2007;292:H884–892 [PubMed: 17012350]

44. Suo J, Ferrara DE, Sorescu D, Guldberg RE, Taylor WR, Giddens DP. Hemodynamic shear stresses in mouse aortas: Implications for atherogenesis. Arterioscler. Thromb. Vasc. Biol 2007;27:346–351 [PubMed: 17122449]

45. Kelly Donovan OA, Qi Xin, Cho William, and Azizkhan-Clifford1 Jane. O-glcnac modification of transcription factor sp1 mediates hyperglycemia-induced vegf-a upregulation in retinal cells. Invest Ophthalmol Vis Sci. 2014;55:7862–7873 [PubMed: 25352121]

46. Cheung WD, Hart GW. Amp-activated protein kinase and p38 mapk activate o-glcnacylation of neuronal proteins during glucose deprivation. J. Biol. Chem 2008;283:13009–13020 [PubMed: 18353774]

47. Alexander Golks T-TTT, Goetschy Jean Francois and Guerini Danilo. Requirement for o-linked n-acetylglucosaminyltransferase in lymhocytes activation. EMBO 2007;26

48. Hilgers RH, Xing D, Gong K, Chen YF, Chatham JC, Oparil S. Acute o-glcnacylation prevents inflammation-induced vascular dysfunction. Am. J. Physiol. Heart Circ. Physiol 2012;303:H513–522 [PubMed: 22777418]

49. Hanover JA. Glycan-dependent signaling: O-linked n-acetylglucosamine. The FASEB Journal. 2001;15:1865–1876 [PubMed: 11532966]

50. Wang L, Luo JY, Li B, Tian XY, Chen LJ, Huang Y, Liu J, Deng D, Lau CW, Wan S, Ai D, Mak KK, Tong KK, Kwan KM, Wang N, Chiu JJ, Zhu Y, Huang Y. Integrin-yap/taz-jnk cascade mediates atheroprotective effect of unidirectional shear flow. Nature. 2016;540:579–582 [PubMed: 27926730]

51. Bertero T, Oldham WM, Cottrill KA, Pisano S, Vanderpool RR, Yu Q, Zhao J, Tai Y, Tang Y, Zhang YY, Rehman S, Sugahara M, Qi Z, Gorcsan J 3rd, Vargas SO, Saggar R, Saggar R, Wallace WD, Ross DJ, Haley KJ, Waxman AB, Parikh VN, De Marco T, Hsue PY, Morris A, Simon MA, Norris KA, Gaggioli C, Loscalzo J, Fessel J, Chan SY. Vascular stiffness mechanoactivates yap/taz-dependent glutaminolysis to drive pulmonary hypertension. J. Clin. Invest 2016;126:3313–3335 [PubMed: 27548520]

52. Kim J, Kim YH, Kim J, Park DY, Bae H, Lee DH, Kim KH, Hong SP, Jang SP, Kubota Y, Kwon YG, Lim DS, Koh GY. Yap/taz regulates sprouting angiogenesis and vascular barrier maturation. J. Clin. Invest 2017;127:3441–3461 [PubMed: 28805663]

53. Liu T-W, Zandberg WF, Gloster TM, Deng L, Murray KD, Shan X, Vocadlo DJ. Metabolic inhibitors of o-glcnac transferase that act in vivo implicate decreased o-glcnac levels in leptin-mediated nutrient sensing. Angewandte Chemie International Edition. 2018;57:7644–7648 [PubMed: 29756380]

54. Sobhakumari A, Orcutt KP, Love-Homan L, Kowalski CE, Parsons AD, Knudson CM, Simons AL. 2-deoxy-d-glucose suppresses the in vivo antitumor efficacy of erlotinib in head and neck squamous cell carcinoma cells. Oncol. Res 2016;24:55–64 [PubMed: 27178822]

55. Guo ZH, Mattson MP. In vivo 2-deoxyglucose administration preserves glucose and glutamate transport and mitochondrial function in cortical synaptic terminals after exposure to amyloid beta-peptide and iron: Evidence for a stress response. Exp. Neurol 2000;166:173–179 [PubMed: 11031093]

56. Goldberg L, Israeli R, Kloog Y. Fts and 2-dg induce pancreatic cancer cell death and tumor shrinkage in mice. Cell Death &Amp; Disease. 2012;3:e284

57. Huang C-C, Wang S-Y, Lin L-L, Wang P-W, Chen T-Y, Hsu W-M, Lin T-K, Liou C-W, Chuang J-H. Glycolytic inhibitor 2-deoxyglucose simultaneously targets cancer and endothelial cells to suppress neuroblastoma growth in mice. Disease Models &amp; Mechanisms. 2015;8:1247 [PubMed: 26398947]

58. Eguchi S, Oshiro N, Miyamoto T, Yoshino K, Okamoto S, Ono T, Kikkawa U, Yonezawa K. Amp-activated protein kinase phosphorylates glutamine : Fructose-6-phosphate amidotransferase 1 at ser243 to modulate its enzymatic activity. Genes Cells. 2009;14:179–189 [PubMed: 19170765]

59. Chiu J-J, Chien S. Effects of disturbed flow on vascular endothelium: Pathophysiological basis and clinical perspectives. Physiol. Rev 2011;91:327–387 [PubMed: 21248169]

60. Rothlein R, Wegner C. Role of intercellular adhesion molecule-1 in the inflammatory response. Kidney Int. 1992;41:617–619 [PubMed: 1349363]

61. Brenner JS, Kiseleva RY, Glassman PM, Parhiz H, Greineder CF, Hood ED, Shuvaev VV, Muzykantov VR. The new frontiers of the targeted interventions in the pulmonary vasculature: Precision and safety (2017 grover conference series). Pulmonary circulation. 2017;8:2045893217752329–2045893217752329 [PubMed: 29261028]

62. Du X, Matsumura T, Edelstein D, Rossetti L, Zsengeller Z, Szabo C, Brownlee M. Inhibition of gapdh activity by poly(adp-ribose) polymerase activates three major pathways of hyperglycemic damage in endothelial cells. J. Clin. Invest 2003;112:1049–1057 [PubMed: 14523042]

63. Beleznai T, Bagi Z. Activation of hexosamine pathway impairs nitric oxide (no)-dependent arteriolar dilations by increased protein o-glcnacylation. Vascul. Pharmacol 2012;56:115–121 [PubMed: 22155161]

64. Aulak KS, Barnes JW, Tian L, Mellor NE, Haque MM, Willard B, Li L, Comhair SC, Stuehr DJ, Dweik RA. Specific o-glcnac modification at ser-615 modulates enos function. Redox Biol. 2020;36:101625 [PubMed: 32863226]

65. Tashima Y, Stanley P. Antibodies that detect o-linked beta-d-n-acetylglucosamine on the extracellular domain of cell surface glycoproteins. J. Biol. Chem 2014;289:11132–11142 [PubMed: 24573683]

66. Zeng Y, Tarbell JM. The adaptive remodeling of endothelial glycocalyx in response to fluid shear stress. PLoS One. 2014;9:e86249 [PubMed: 24465988]

67. van den Berg BM, Spaan JA, Rolf TM, Vink H. Atherogenic region and diet diminish glycocalyx dimension and increase intima-to-media ratios at murine carotid artery bifurcation. Am. J. Physiol. Heart Circ. Physiol 2006;290:H915–920 [PubMed: 16155109]

68. Yehezkel G, Cohen L, Kliger A, Manor E, Khalaila I. O-linked beta-n-acetylglucosaminylation (o-glcnacylation) in primary and metastatic colorectal cancer clones and effect of n-acetyl-beta-d-glucosaminidase silencing on cell phenotype and transcriptome. J. Biol. Chem 2012;287:28755–28769 [PubMed: 22730328]

**NOVELTY AND SIGNIFICANCE**

**What Is Known?**

- A hallmark of atherosclerosis is endothelial cell dysfunction, characterized by the decreased production of nitric oxide.

- In areas where laminar flow becomes disturbed, such as arterial curvatures or bifurcations, endothelial cells produce less nitric oxide.

- Endothelial nitric oxide synthase (eNOS), the enzyme that produces nitric oxide, becomes GlcNAcylated in diabetes, which reduces nitric oxide production.

**What New Information Does This Article Contribute?**

- Endothelial cells cultured in conditions of laminar flow had almost no eNOS GlcNAcylation and produced more nitric oxide compared to endothelial cells cultured in disturbed flow, which demonstrated increased eNOS O-GlcNAcylation and lower levels of nitric oxide.

- Laminar flow reduced endothelial cell eNOS O-GlcNAcylation by decreasing glycolysis.

- When glycolysis was inhibited in endothelial cells exposed to disturbed flow, the cells decreased eNOS O-GlcNAcylation and produced more nitric oxide.
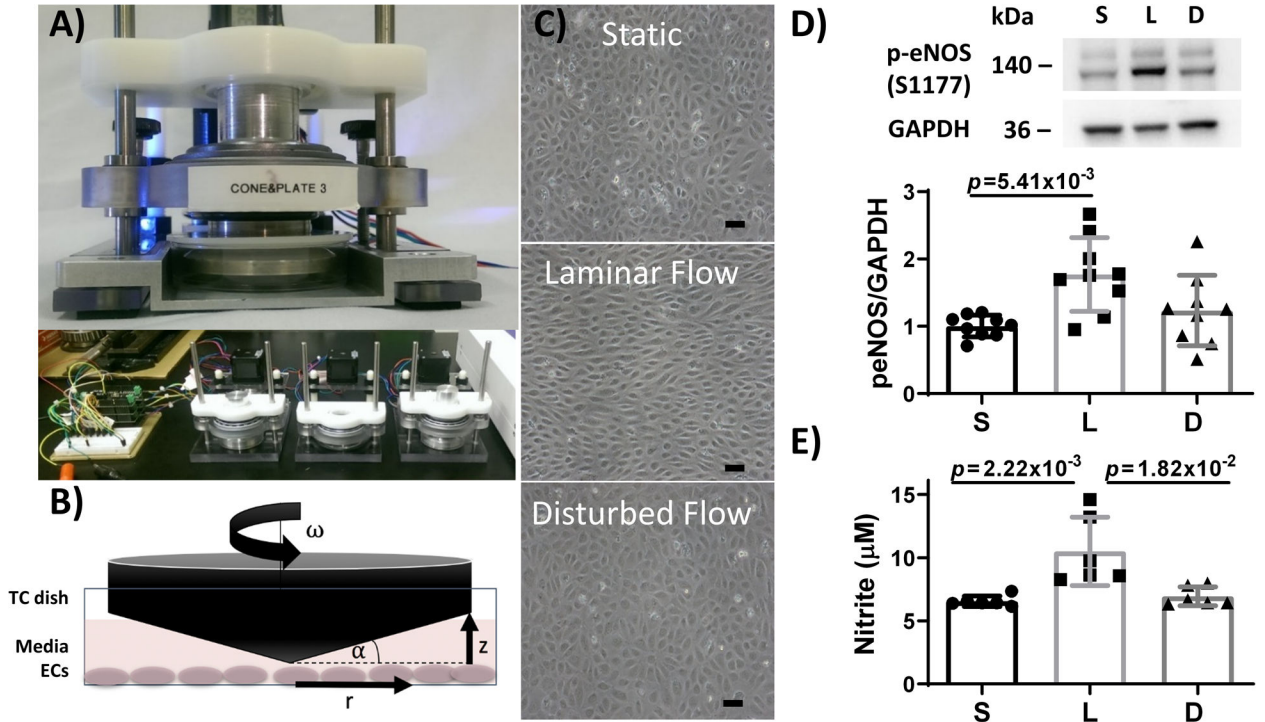
**Figure 1: Endothelial cells (ECs) exposed to steady laminar flow via custom cone-and-plate device elongated and aligned with the flow direction, phosphorylated more eNOS, and produced more nitric oxide (NO) than ECs exposed to static culture or oscillating disturbed flow.**
(A) Custom-built cone and plate device designed to expose 3 parallel yet independent samples to flow. (B) Diagram of the cone and plate system, where r is radial distance from the cone apex, $\omega$ is cone angular velocity, $\alpha$ is cone angle, and z is vertical distance between the cone and plate. TC = tissue culture. (C) Representative phase contrast images of HUVEC exposed to static culture, steady laminar flow, or oscillating disturbed flow for 24 hours. Scale bar = 50 μm. (D) Western blot of phosphorylated eNOS (p-eNOS) and GAPDH in HUVEC adapted to static culture (S), steady laminar flow (L), or oscillating disturbed flow (D) for 24 hours. n = 9 samples, normalized to static culture and GAPDH. $p = 1.00 \times 10^{-2}$ by Kruskal-Wallis test, with p value on the figure determined by Dunn's multiple comparisons test (all samples compared to steady laminar flow). (E) NO, measured via Griess Assay, increased in HUVEC adapted to steady laminar flow but not oscillating disturbed flow for 24 hours. n = 6 samples per experiment. 1 representative experiment shown out of 2 total experiments. $p = 2.10 \times 10^{-4}$ by Kruskal-Wallis test, with p values on the figure determined by Dunn's multiple comparisons test (all samples compared to steady laminar flow).
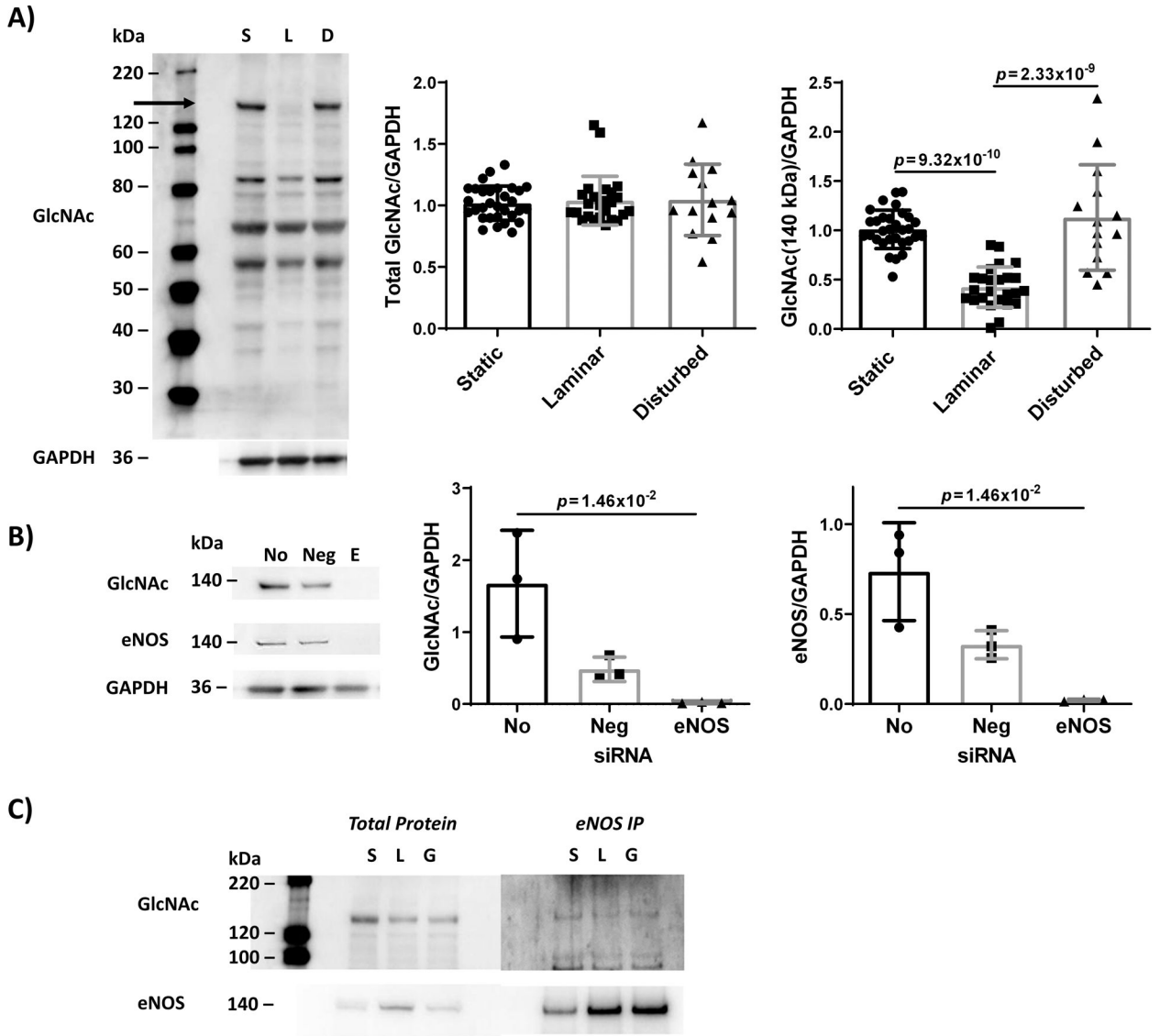
**Figure 2. Steady laminar flow, but not oscillating disturbed flow, decreased EC eNOS O-GlcNAcylation.**

(A) Western blot for all O-GlcNAcylated proteins, with quantification of total GlcNAcylated proteins and GlcNAcylation of the ~140 kDa protein only (indicated by arrow). Confluent HUVEC were first adapted to static culture ('S'), steady laminar ('L', 20 dynes/cm2), or oscillating disturbed flow ('D', $4\pm6$ dynes/cm$^2$) for 24 hrs. n = 14 – 31 samples, normalized to static culture and GAPDH. For GlcNAc-eNOS, p = $1.84\times10^{-11}$ by one-way ANOVA, with p values on the figure determined by Tukey's multiple comparisons test. (B) Western blot for all O-GlcNAcylated proteins and total eNOS for HUVEC with eNOS knocked down via siRNA. Quantification of GlcNAcylation of the ~140 kDa protein and total eNOS. (No: HUVEC without siRNA; Neg: control siRNA; E: eNOS siRNA). n = 3 samples. For GlcNac/GAPDH and eNOS/GAPDH, p = $3.57\times10^{-3}$ by Kruskal-Wallis test, with p values on the figure determined by Dunn's multiple comparisons test (all samples compared to "No"). (C) Western blot for all O-GlcNAcylated proteins and total eNOS for HUVEC
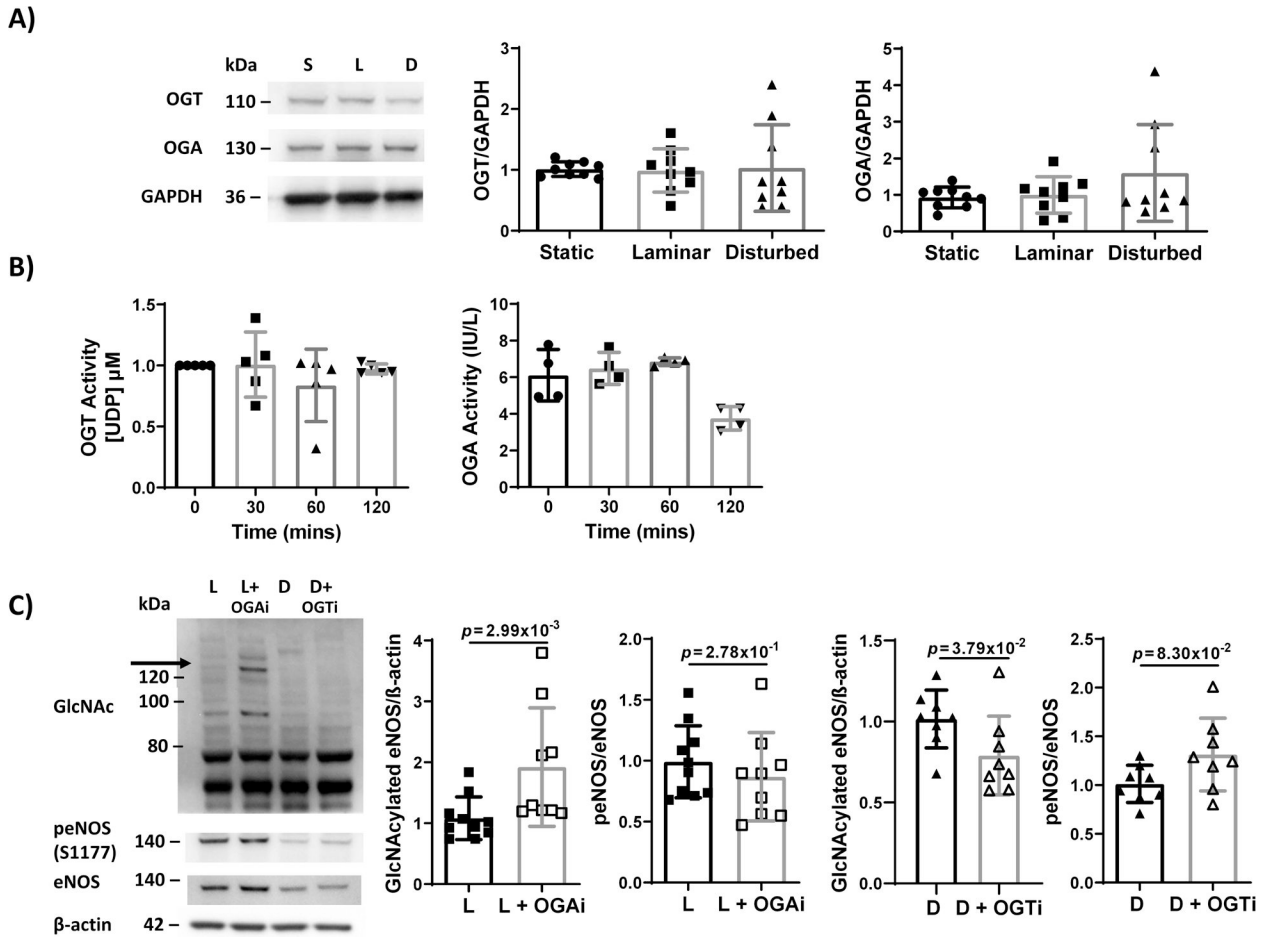
after eNOS immunoprecipitation. Static 'S', steady laminar 'L', 3 hour 5 mM glucosamine 'G'. 3 independent samples were combined into 1 sample to obtain enough protein for immunoprecipitation.

A)



B)



C)



**Figure 3: OGT and OGA quantity and activity did not significantly change with flow. OGT inhibition in cells exposed to disturbed flow decreased eNOS O-GlcNAcylation and increased eNOS phosphorylation, while OGA inhibition in cells exposed to laminar flow increased eNOS O-GlcNAcylation and decreased eNOS phosphorylation.**

(A) Western blot and quantification of OGT and OGA in HUVECs exposed to 24 hours static culture ('S'), steady laminar ('L'), or oscillating disturbed flow ('D'). n = 9 samples, normalized to static culture and GAPDH. (B) OGT and OGA activity assay of HUVECs exposed to 0, 30, 60, 120 minutes steady laminar flow. n = 4–5 samples. For OGA, p = $1.17 \times 10^{-2}$ by Kruskal-Wallis test. (C) Western blot and quantification of eNOS O-GlcNAcylation and p-eNOS in HUVECs exposed to 24 hours steady laminar flow +/− 1:1000 OGA inhibitor ('L', 'L+OGAi') or oscillating disturbed flow +/− 1:1000 OGT inhibitor ('D', 'D+OGTi'). n = 8–10 samples, normalized to untreated and βactin. p values on the figure determined by Mann-Whitney test.
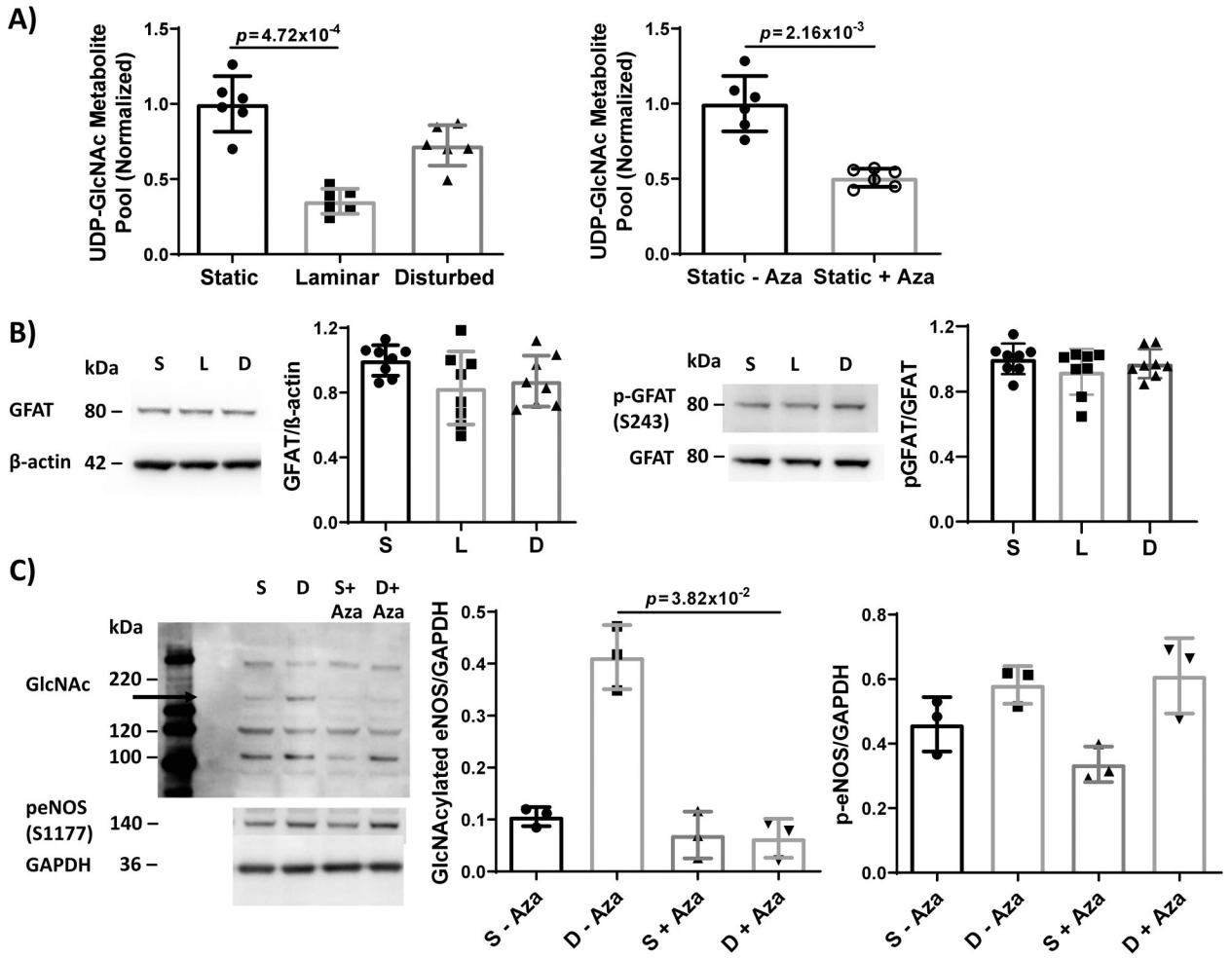
**Figure 4: HBP flux and UDP-GlcNAc substrate decreased in HUVEC exposed to steady laminar flow without a change in GFAT. GFAT inhibition decreased UDP-GlcNAc, and in cells exposed to disturbed flow, decreased eNOS O-GlcNAcylation and increased eNOS phosphorylation.**

(A) UDP-GlcNAc total metabolite pool measured by mass spectrometry in HUVEC exposed to 24 hours static culture, steady laminar, or oscillating disturbed flow or HUVEC exposed to 24 hours static culture with and without 1 μM azaserine (+/− Aza, GFAT inhibitor). Total pool was normalized to the average pool size for static, untreated cells. n = 6 samples per condition. For flow conditions, p = $9.79\times10^{-6}$ by Kruskal-Wallis test, with p value on the figure determined by Dunn's multiple comparisons test. For azaserine treatment, p value on the figure determined by Mann-Whitney test. (B) Western blot and quantification of GFAT and p-GFAT (S243) in HUVECs exposed to 24 hours static culture, steady laminar, or oscillating disturbed flow. n = 8 samples, normalized to static cultured and βactin or GFAT. p = $1.26\times10^{-1}$ (GFAT) and p = $4.70\times10^{-1}$ (p-GFAT) by Kruskal-Wallis test. (C) Western blot and quantification of protein O-GlcNAcylation and p-eNOS in HUVECs exposed to static culture ('S') or 24 hours oscillating disturbed flow ('D') with and without 1 μM azaserine (+/− Aza, GFAT inhibitor). n = 3 samples. p = $2.34\times10^{-2}$ (GlcNAc eNOS) and p = $3.39\times10^{-2}$ (p-eNOS) by Kruskal-Wallis test, with p values on the figure determined by Dunn's multiple comparisons test.
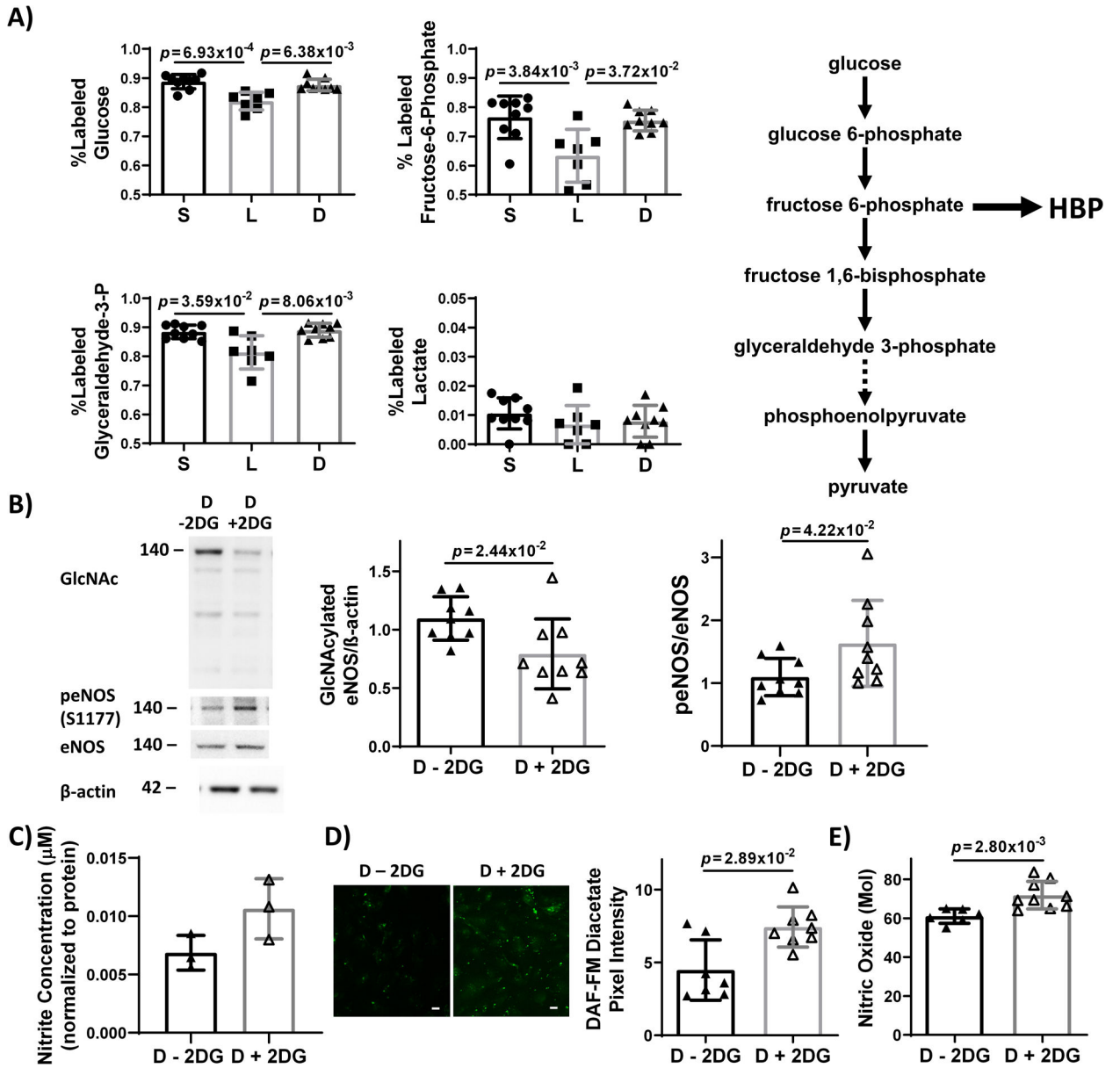
**Figure 5: Glycolytic flux decreased in EC exposed to steady laminar flow as compared to static culture and oscillating disturbed flow. Inhibiting glycolysis via 2-DG in EC exposed to oscillating disturbed flow decreased eNOS O-GlcNAcylation and subsequently increased eNOS phosphorylation and NO.**

(A) % labeled intracellular glycolytic intermediates (glucose, fructose-6-phosphate, glyceraldehyde-3-phosphate, and lactate) measured by mass spectrometry in HUVEC exposed to 24 hours static culture ('S'), steady laminar ('L'), or oscillating disturbed flow ('D') followed by $^{13}C$-glucose for 2 minutes. A simplified glycolysis pathway is depicted showing glucose metabolized to pyruvate, which is then converted to lactate. The hexosamine biosynthetic pathway (HBP) branches off glycolysis at fructose-6-phosphate. n = 9 samples, normalized to static culture and βactin or eNOS. p = $8.75 \times 10^{-4}$ (glucose), p = $6.19 \times 10^{-3}$ (fructose-6-phosphate), and p = $1.06 \times 10^{-2}$ (glyceraldehyde-3-phosphate) by Kruskal-Wallis test, with p values on the figure determined by Dunn's multiple comparisons

test. (B) Western blot and quantification of eNOS O-GlcNAcylation and p-eNOS in HUVECs exposed to 24 hours oscillating disturbed flow +/− 1 μM 2-DG. n = 9 samples. Statistical significance determined by Mann-Whitney test. (C) NO levels, measured via Griess Assay, in HUVEC exposed to 24 hours oscillating disturbed flow +/− 1 μM 2-DG. n = 3 samples per experiment. 1 representative experiment shown of 3 total experiments. (D) DAF-FM diacetate fluorescent images (green) and quantification of intracellular NO in HUVEC exposed to 24 hours oscillating disturbed flow +/− 1 μM 2-DG. Scale bar = 20 μm. n = 7 samples. 1 representative experiment shown of 2 total experiments. Statistical significance determined by Mann-Whitney test. E) Zysense NO analyzer quantification of NO in the conditioned media from HUVEC exposed to 24 hours oscillating disturbed flow +/− 1 μM 2-DG. n = 6 samples 1 representative experiment shown of 2 total experiments. Statistical significance determined by Mann-Whitney test.

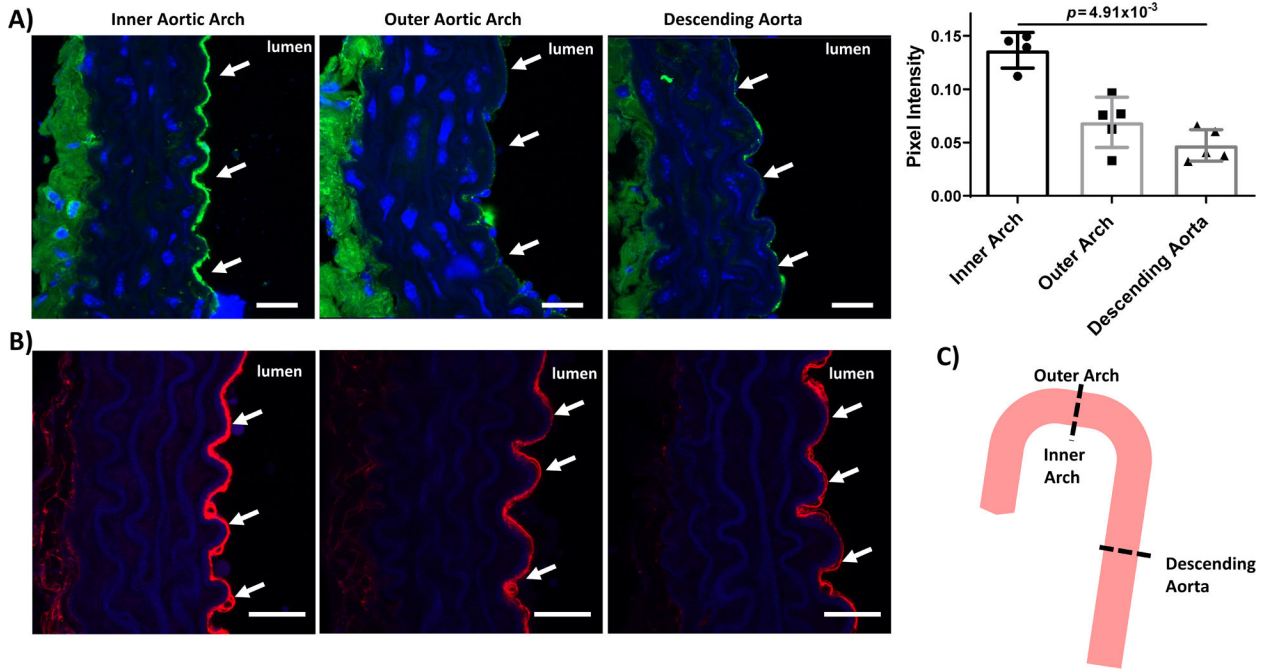**Figure 6: Endothelium in the inner aortic arch showed increased protein O-GlcNAcylation as compared to endothelial cells in the outer aortic arch and descending aorta.**
Confocal microscopy images of inner and outer aortic arch and descending aorta cross sections from 2-month-old male C57BL/6J mice labeled for (A) O-GlcNAcylated proteins (green) and (B) ICAM-1 (red). Blue = nuclei. Scale bar = 20 μm. White arrows highlight the endothelium. Also shown is quantification of green pixel intensity in the endothelium. n = 4–5 samples. p = $1.60\times10^{-3}$ by Kruskal-Wallis test, with p value on the figure determined by Dunn's multiple comparisons test (all samples compared to inner arch).(C) Schematic of mouse aorta cross-sections. Outer aortic arch and descending aorta endothelium are exposed to laminar flow whereas inner aortic arch endothelium is exposed to disturbed flow.